



Since January 2020 Elsevier has created a COVID-19 resource centre with free information in English and Mandarin on the novel coronavirus COVID-19. The COVID-19 resource centre is hosted on Elsevier Connect, the company's public news and information website.

Elsevier hereby grants permission to make all its COVID-19-related research that is available on the COVID-19 resource centre - including this research content - immediately available in PubMed Central and other publicly funded repositories, such as the WHO COVID database with rights for unrestricted research re-use and analyses in any form or by any means with acknowledgement of the original source. These permissions are granted for free by Elsevier for as long as the COVID-19 resource centre remains active.



Retinal findings of COVID-19 patients using ocular coherence tomography angiography two to three months after infection[☆]

Ocular appearance recovered COVID-19 patient

Afsaneh Naderi Beni^{a,*}, Alireza Dehghani^a, Farzan Kianersi^a, Heshmatollah Ghanbari^a, Zahra Habibidastena^b, Seyed Ezatollah Memarzadeh^b, Zahra Naderi Beni^b

^a Isfahan Eye Research Center, Department of ophthalmology, Isfahan University of medical sciences, Isfahan, Iran

^b Shahrekord university of medical sciences, Iran

ARTICLE INFO

Keywords:

Ocular finding retinal finding
COVID-19
Optical coherence tomography angiography

ABSTRACT

Purpose: The aim of this study was to evaluate the ocular disorders in COVID-19 patients, two to three months after infection.

Methods: In this cross-sectional, historically controlled study, fifty-one COVID-19 patients were compared with thirty-seven age, and gender-matched healthy individuals. After complete ophthalmological examination, all participants underwent peripapillary and macular optical coherence tomography, and optical coherence tomography angiography (OCTA) measurements (OptoVue Inc, Freemont, CA, USA).

Results: The time between the initial onset of symptoms, and ophthalmologic examination was 63.31 ± 15.21 (40–95 days). Ophthalmic examination of all the recovered COVID-19 patients was within normal range. None of the peripapillary and macular OCTA parameters were significantly different between the two groups with pairwise comparisons, but after adjusting for age, gender, axial length, and signal strength index (SSI), recovered COVID-19 eyes showed a significant increase in peripapillary retinal nerve fiber (RNFL) thickness, superficial, and deep macular vessel densities in parafoveal and perifoveal regions compared with healthy control eyes ($p < 0.05$). Inner retinal thickness overall is higher in recovered COVID-19 eyes compared to healthy eyes after adjustment.

Conclusion: Patients with moderate-intensity SARS-CoV-2 pneumonia had altered peripapillary and macular vessel density compared to healthy subjects. Further investigation is warranted to analyze the correlation of these changes with disease severity as well as evolution of these changes over time.

1. Background

Coronavirus disease 2019 (COVID-19) has quickly spread around the world, affecting various parts of the human body, and ophthalmological manifestations are associated with extraocular disease, such as conjunctivitis [1].

Optical coherence tomography (OCT) and optical coherence

tomography angiography (OCT-A) are non-invasive methods to establish retinal changes, as well as visualization of both perfused vascular network and vascular abnormalities without the use of the contrast-enhancing drugs. Some studies reported the retinal finding of COVID-19 in the acute phase, and after recovery [2–10].

To the best of our knowledge, there are few reports on the effects of COVID-19 in the eye during the months, after infection; hence, the aim

Abbreviations: OCTA, Optical coherence tomography angiography; SSI, signal strength index; RNFL, retinal nerve fiber layer; OCT, Optical coherence tomography; SpO₂, oxygen saturation; CDC, the Centers for Disease Control and Prevention; BCVA, Best-corrected visual acuity; VD, vessel density; ILM, internal limiting membrane; DCP, deep capillary plexus; INL, the inner nuclear layer; OPL, outer plexiform layer; FAZ, . foveal avascular zone; SCP, superficial capillary plexus; AI, acircularity index; ONH, Optic Nerve Head; GCC, ganglion cell complex; SD, standard deviation; RT-PCR, reverse transcription Polymerase Chain Reaction; VA, Visual acuity; SVD, superficial vessel density; DVD, deep vessel density; ACE, Angiotensin-converting enzyme; ICU, inhibitors, intensive care unit; FD, foveal vessel density; CNS, central nervous system; HIF-1, hypoxia-inducible factor 1; VEGFA, vascular endothelial growth factor A.

[☆] The authors do not have any financial interest in any products mentioned in this article.

* Corresponding author at: Feiz hospital, Ophthalmology department, Modares Street, Iran.

E-mail address: a_naderibeni@yahoo.com (A. Naderi Beni).

<https://doi.org/10.1016/j.pdpdt.2022.102726>

Received 13 November 2021; Received in revised form 10 January 2022; Accepted 14 January 2022

Available online 17 January 2022

1572-1000/© 2022 Elsevier B.V. All rights reserved.

was to systematically evaluate the ocular involvement, using routine examination as well as OCT and OCT angiography amongst the recovered COVID-19 patients.

2. Materials & methods

This cross-sectional, historically controlled study was conducted in the Ophthalmology department of Feiz Hospital, which is a referral center affiliated with Isfahan University of Medical Sciences, Iran, as well as Shahrekord University of Medical Sciences, Iran, from March 2020 till June 2020. Fifty-one eyes of the 51 hospitalized patients after they had recovered from COVID-19 infection, and 37 eyes of age and gender-matched healthy individuals were compared. Prior to entering the study, and after explaining the study objectives, written informed consent was obtained from the participants. The study protocol was approved, and reviewed by the institutional ethics committee of Isfahan University of Medical Sciences (IR.MUL.MED.REC.1398.105), and it was performed according to the Declaration of Helsinki and its later amendments.

The patients with moderate intensity SARS-CoV-2 pneumonia (individuals who show evidence of lower respiratory disease during clinical assessment or imaging and who have an oxygen saturation (SpO_2) $\geq 94\%$ on room air at sea level) were enrolled in this study.

All patients received supportive therapy, antiviral treatment, including hydroxychloroquine or and chloroquine phosphate along with Kaletra (lopinavir/ ritonavir), for 5–14 days. Antibiotics and methylprednisolone used for some patients. None of the patients have been vaccinated for COVID-19. According to the Centers for Disease Control and Prevention (CDC), “recovered” means that a person must be fever-free without fever-reducing medications for three consecutive days, and they must show an improvement in respiratory symptoms like cough, shortness of breath; and, at least 7–10 days have passed since symptoms began. Also, a person had two consecutive negative coronavirus tests, which should be taken at least 24 h apart.

All eligible participants underwent a comprehensive ophthalmologic examination, including Best-corrected visual acuity (BCVA) measurement, slit-lamp biomicroscopy, IOP measurement with Goldmann applanation tonometry, axial length measurement, and dilated fundus examination.

The historical control group included healthy individuals aged 10 to 70 years old. Ophthalmology examination, OCT, and OCT angiography were performed before the outbreak of the COVID-19 virus, and maintained as the normal database in our center.

Controls were obtained from a large OCTA database at Feiz Hospital (Isfahan, Iran) from the previous study [11], and research projects before the COVID-19 pandemic.

Inclusion criteria for the study groups were best-corrected visual acuity (BCVA) of 20/40 or better, and a refractive sphere between -5 and $+3$ diopters, and a refractive cylinder within -3 diopters.

Exclusion criteria included intraocular surgery (except for uncomplicated cataract extraction), history of retinal disease, glaucomatous and non-glaucomatous optic neuropathy, uveitis, or ocular trauma, and other ocular or systemic diseases known to affect the eyes such as vascular diseases, diabetes mellitus, rheumatic diseases. Participants with poor quality of OCT and OCT-A scans were excluded from the study. If both eyes were eligible, only one eye was randomly selected for analysis.

3. OCT-A image acquisition and processing

The OCTA scans were obtained, using RTVue-XR spectral domain OCT (AngioVue, Optovue Inc., Fremont, California, USA; version 2017.1.0.151). A $4.5 \times 4.5 \text{ mm}^2$ area centered on the optic disk was used for optic disk scan; while a $3 \times 3 \text{ mm}^2$, and a $6 \times 6 \text{ mm}^2$ area centered on the fovea was used for the macular scan. During the screening process, different layers of retinal vascular networks were observed. The ratio of

the area occupied by vessels divided by the total area was defined as vessel density (VD).

A blood vessel was defined as pixels having decorrelation values two standard deviations above the threshold level (two standard deviations above noise).

In the optic disk scan, the whole image VD an area scan of $4.5 \times 4.5 \text{ mm}^2$, average VD within the ONH (inside disk VD), and peripapillary VD (measured in a 750 μm -wide annulus extending outward from the optic disk boundary) were calculated automatically by software.

The peripapillary VD was analyzed from the radial peripapillary capillary segment, extending from the internal limiting membrane (ILM) to the posterior boundary of the RNFL. The peripapillary region was divided into eight sectors, every 45° . An experienced OCTA technician performed all the OCTA examinations.

In the macular scan three-dimensional OCTA scans were acquired over $3 \times 3 \text{ mm}^2$ and $6 \times 6 \text{ mm}^2$ regions. Macular vessel densities analyzed in this study were of the superficial vascular plexus (span from the ILM to the lower border of IPL) and deep capillary plexus (DCP) (span from the inner nuclear layer (INL) to the outer plexiform layer (OPL)).

The angio-retina scans were automatically inserted in three concentric circles at the fovea with diameters of 1, 3, and 6 mm. The small circular area with a diameter of 1 mm was defined as the foveal zone. The area between the inner (1-mm) and middle (3-mm) rings was considered parafovea, and the perifovea was defined area between the 3 and 6 mm radius.

The parafoveal and perifoveal regions were automatically divided into two sectors of 180° each (superior and inferior sectors), and four quadrants: the superior, inferior, temporal, and nasal quadrants.

Parafoveal and perifoveal values were calculated, using the average vessel density of the four quadrants. Measurement of the foveal avascular zone (FAZ) area in the superficial capillary plexus (SCP) was obtained, using the non-flow assessment tool, and the FAZ area, including the full retinal vasculature, FAZ perimeter, acircularity index (AI) of the FAZ, and foveal density-300, which were measured, using the FAZ assessment tool. In addition, retinal thickness was derived from the optical coherence tomography (OCT) images.

From the participant data, one eye was randomly selected for the statistical analysis.

Images with lower quality (signal strength index [SSI] < 45), Segmentation errors due to artifacts, or any residual motion artifacts were excluded. The RNFL thickness measurement was generated at 3.45-mm-diameter circle relative to the disk center for each sector on the ONH map, and macular ganglion cell complex (GCC) thickness was measured from the internal limiting membrane (ILM) to the outer inner plexiform layer (IPL) boundary in the superior, inferior hemiretina, and overall GCC map.

3.1. Statistical analysis

Statistical analyses were performed, using the statistical software SPSS, version 22 (SPSS, Inc., Chicago, IL, USA). P values < 0.05 were considered to be statistically significant. Continuous variables are expressed as mean \pm standard deviation. Categorical data were reported as numbers (percentages). The distribution of numerical data was tested for normality, using the Kolmogorov–Smirnov test. Independent samples *t*-test was used to compare the vessel density between groups. The two-tailed statistical significance of Pearson’s correlation coefficient was used to test the correlation between different parameters. Multi-variable analysis was done to adjust for age, gender, axial length, and SSI of the image. $P < 0.05$ was considered statistically significant

4. Results

In this study, fifty-one eyes from 51 COVID-19 patients two–three months after infection were compared with thirty-seven eyes of 37 healthy participants (Tables 1, and 2). In total, 53 (60.22%) were male,

Table 1
Demographic Details, Clinical Characteristics, and Lab data of patients in acute phase of COVID-19 disease. F= Female, M= Male.

Duration of onset of disease to the study (days)	WBC	PLT	Rdw-sd	Rdw-cv	RBC	NEUTcount	MXD	MCV	MCH	MCHC	LymphCount	LDH	Hb	HCT	CRP	ESR	Ca	Clinical symptom	Sex	Age	
60	6100	305,000	38.1	12.2	5.19	3.2	0.6	86.5	31.2	36.1	2.3	-	16.2	44.9	6	16	9.0	Cough Fatigue	F	35	1
95	11,000	166,000	47.0	12.9	4.84	7.4	1.3	92.1	33.1	35.9	2.3	-	16.0	44.6	-	18	8.9	Vomiting Fever Cough Dyspnea	F	9	2
90	9900	281,000	41.3	12.9	5.06	6.0	0.7	85.6	31.2	36.5	3.2	-	15.8	43.3	-	-	-	vomiting Fever	M	25	3
62	3400	135,000	42.0	12.6	4.7	2.7	0.1	87.7	31.1	35.4	0.6	-	14.6	41.2	-	64	8.3	Myalgia Fever Dyspnea	M	45	4
74	3600	164,000	42.6	12.8	3.85	2.0	0.3	88.4	31.9	36.1	1.2	-	14.5	40.2	17	73	8.6	Fatigue Myalgia Fever	F	67	5
74	12,200	146,000	45.7	20.1	3.77	10.6	0.4	64.5	18.6	28.8	1.2	-	7.0	24.3	18	40	7.2	Dyspnea Fever Cough	F	67	6
60	8200	207,000	46.7	14.7	4.95	0.0	0.2	87.8	25.3	29.0	1.6	1472	12.8	46.6	-	-	8.3	Fatigue Fever Cough	F	34	7
62	6600	241,000	42.5	13.1	4.88	3.3	0.4	84.0	27.0	32.2	2.9	-	13.2	41.0	8	11	-	Dyspnea Fatigue myalgia	M	32	8
76	10,900	101,000	51.8	14.9	2.84	9.3	0.8	96.5	32.7	33.9	0.8	521	9.3	27.4	15	91	-	diarrhea Fever Diarrhea	M	38	9
40		840,000	52.9	15.4	3.53	28.1	0.4	89.3	31.8	34.9	1.0	606	13.0	37.3	-	86		Headache diarrhea	M	48	10
75	12,900	109,000	46.1	13.6	4.34	9.4	1.2	88.0	29.7	33.8	2.3	-	12.9	38.2	-	17	8.5	Fever Dyspnea Fatigue	M	51	11
64	21,600	290,000	48.9	13.9	5.32	5.3	13.5	93.6	32.5	34.7	2.8	-	17.3	49.8	1	44	9.3	headache Fever Cough	M	48	12
60	8200	277,000	47.3	13.6	4.26	4.9	1.0	93.4	32.2	34.4	2.3	-	13.7	39.8	8	25	9.1	Dyspnea Fatigue Myalgia	F	26	13
73	10,100	175,000	42.6	13.1	4.77	8.2	0.3	87.8	27.5	31.3	1.6	-	13.1	41.9	-	16	8.2	vomiting diarrhea Fever	M	35	14
95	6600	352,000	40.8	13.1	5.41	5.2	0.2	82.8	29.6	35.7	1.2		16.0	44.8	8			Dyspnea Fatigue Myalgia	F	12	15
95	5600	239,000	42.0	13.4	4.93		0.5	81.6	28.8	35.6	2.1	748	15.4	43.6	-	30	8.6	headache Fever myalgia	M	33	16

(continued on next page)

Table 1 (continued)

Duration of onset of disease to the study (days)	WBC	PLT	Rdwsd	Rdwc	RBC	NEUTcount	MXD	MCV	MCH	MCHC	LymphCount	LDH	Hb	HCT	CRP	ESR	Ca	Clinical symptom	Sex	Age	
90	18,400	241,000	42.9	12.9	3.94	15.3	0.7	86.8	31.0	35.7	2.4	1065	12.2	34.2	-	-	7.8	Vomiting headache Fever Cough Dyspnea	M	25	17
60	5900	271,000	49.4	14.5	3.79	3.7	0.2	93.4	34.0	36.4	2.0	-	12.9	35.4	-	32	8.9	headache Fever Dyspnea Chest pain	F	41	18
76	9200	361,000	47.4	14.8	4.02	6.0	1.3	86.1	27.4	31.8	1.9	-	11.0	34.6	-	123	-	Fatigue	M	38	19
95	8100	470,000	43.8	14.1	4.98	0.0	0.0	81.7	28.3	35.2	0.7	-	14.7	42.9	-	28	8.4	Fever Dyspnea	M	31	20
62	6700	138,000	45.9	13.3	5.06	3.9	0.6	89.9	31.2	34.7	2.2	-	15.8	45.5	-	-	-	Fever Dyspnea Chest pain	M	32	21
55	5200	174,000	45.9	13.2	4.73	3.9	0.2	89.4	32.6	36.4	1.1	501	15.4	42.3	4	19	8.8	Fever Dyspnea	M	25	22
44	12,000	158,000	40.4	12.8	4.14	10.1	0.6	86.5	29.7	34.4	1.3	399	-	35.8	-	80	-	Myalgia headache	M	40	23
55	14,400	128,000	43.2	13.2	3.67	11.6	0.6	85.7	28.4	33.2	2.2	570	12.1	36.5	22	32	-	Fever Cough Dyspnea Fatigue	M	25	24
64	3800	137,000	47.3	12.8	4.12	2.1	0.5	96.6	34.7	35.9	1.2	456	14.3	39.8	4	47	7.9	Fever Dyspnea	M	46	25
50	8500	232,000	43.8	13.5	4.31	6.3	0.6	84.0	24.4	29.0	1.6	-	10.5	36.2	-	32	-	Fever Cough Dyspnea Fatigue	F	28	26
43	8600	74,000	74.1	20.2	5.7	7.1	0.5	99.6	31.1	31.2	1.0	640	17.7	56.8	-	13	8.6	Fever Cough Dyspnea Fatigue	M	51	27
44	5400	169,000	44.7	12.4	4.75	3.9	0.5	89.7	31.4	35.0	1.0	-	14.9	42.6	9	117	8.6	Myalgia headache	M	38	28
42	24,800	137,000	49.9	12.6	4.52	5.5	0.4	96.4	35.9	36.2	4.1	-	16.1	45.0	-	12	-	Fever Cough Dyspnea Fatigue	F	53	29
69	10,600	237,000	49.6	14.4	4.19	9.6	0.2	85.7	26.4	30.5	0.8	-	11.2	35.9	-	-	8.2	Fever Cough Dyspnea Fatigue	F	62	30
69	17,800	270,000	51.3	13.8	3.56	0.0	0.0	97.5	33.4	34.3	1.6	157	11.9	34.7	-	80	8.2	Fever Dyspnea	F	62	31
60	3900	129,000	47.6	17.2	4.28	2.9	0.2	77.3	24.6	32.6	0.7	649	14.7	46.2	19	25	8.0	Fever Dyspnea	F	41	32
43	6700	349,000	47.5	13.1	3.32	6.4	0.0	94.0	32.7	34.1	1.4	609	15.5	46.7	2	66	6.4	Fever Cough Dyspnea Fatigue	M	51	33
60		158,000	49.3	14.0	4.64	3.5	0.4	90.5	33.1	35.8	0.4	425	14.8	42.0	-	11	8.0		F	26	

(continued on next page)

Table 1 (continued)

Duration of onset of disease to the study (days)	WBC	PLT	Rdw-sd	Rdw-cv	RBC	NEUTcount	MXD	MCV	MCH	MCHC	LymphCount	LDH	Hb	HCT	CRP	ESR	Ca	Clinical symptom	Sex	Age	
42	9700	122,000	46.2	14.3	4.52	7.6	0.8	85.2	27.2	31.9	1.3		–	38.5	23	44	8.0	Myalgia headache Fever Cough Dyspnea	F	40	34 35
42	6600	243,000	47.3	14.1	4.65	4.4	0.4	86.7	29.3	33.7	2.9		14.1	41.8	10	27	10.9	Fatigu Myalgia headache	F	50	36
62	4800	109,000	45.9	12.8	4.74	3.0	0.2	93.0	32.1	34.5	1.6	557	15.2	44.1	15	50	8.5	Fever Dyspnea	M	50	37
62	3300	63,000	50.0	16.6	4.39	1.6	0.7	83.5	28.2	33.8	1.5	967	13.2	39.1	–	20	–	Fever Cough Dyspnea Fatigue	M	50	38
62	4400	255,000	42.4	12.6	4.46	3.6	0.1	88.1	28.5	32.3	0.7	1352	12.7	39.3	12.0	96.0	8.0	Fever Cough Dyspnea Fatigue	M	56	39
50	3800	149,000	40.6	12.4	4.55	3.1	0.1	84.8	29.0	34.2	0.6		13.2	38.6	–	17.0	8.0	Fever Cough Dyspnea Fatigue	F	28	40
62	7100	121,000	46.4	12.2	4.52	5.2	0.5	94.7	32.3	34.1	1.4		14.6	42.8	23.0	27.0	8.0	Fever Cough Dyspnea Fatigue	M	44	41
62	7300	169,000	54.0	14.5	5.07	5.3	0.6	97.8	32.5	33.3	1.4	1116	16.5	49.6	9.0	18.0	9.5	Myalgia headache	M	56	42
65	17,400	141,000	49.1	13.8	4.26	15.3	1.2	93.2	33.8	36.3	0.9	–	14.4	39.7	–	27.0	–	Fever Cough Dyspnea Fatigue	M	43	43
65	13,900	205,000	48.7	12.1	3.56	0.0	0.0	102.3	35.7	34.9	3.2	–	12.6	36.1	16.0	24.0	–	Fever Cough Dyspnea Fatigue	M	43	44
62	4700	196,000	50.0	14.7	4.42	3.5	0.1	91.4	25.6	28.0	1.1	–	11.3	40.4	–	25.0	–	Fever Dyspnea	M	44	45
40	16,100	275,000	49.6	19.8	5.62	11.7	1.0	69.0	19.0	27.6	3.4	1346	10.7	38.8	2.0	13.0	8.2	Fever Cough Dyspnea Fatigue	M	48	46
42	16,200	146,000	52.8	16.0	3.68	12.3	1.5	94.3	31.3	33.1	2.4	1509	11.5	34.7	–	45.0	8.9	Fever Cough Dyspnea Fatigue	F	44	47
75	11,900	304,000	49.0	14.1	4.13	8.4	0.6	91.3	31.0	34.0	2.9	458	12.8	37.7	36.0	50.0		Myalgia headache	M	51	48
62	11,900	228,000	52.4	14.8	4.67	8.4	0.5	96.1	33.2	34.5	3.0	371	15.5	44.9	6.0	6.0	9.3	Fever Cough Dyspnea	M	45	49
73	7400	242,000	46.8	13.3	4.45	4.5	0.5	93.5	33.7	36.1	2.4	–	15.0	41.6	–	11.0	9.0		M	35	50

(continued on next page)

Table 1 (continued)

Duration of onset of disease to the study (days)	WBC	PLT	Rdwsd	Rdwcv	RBC	NEUTcount	MXD	MCV	MCH	MCHC	LymphCount	LDH	Hb	HCT	CRP	ESR	Ca	Clinical symptom	Sex	Age	
65	5600	245,000	49.6	16	4.42	4.5	1	96	31	34.5	3	-	12.4	37.8	15	35	7.8	Fever Cough Dyspnea	F	50	51

Calcium = Ca, erythrocyte sedimentation rate = ESR, C-reactive protein = CRP, hematocrit = HCT, Hemoglobin = HB, lactate dehydrogenase = LDH, Lymphocyte count, / μ L = Lymph, mean corpuscular hemoglobin concentration = MCHC, mean cell hemoglobin = MCH. Mean cell volume = MCV, Mixed cell = MXD count, Neutrophil Count $\times 103/\mu$ L = Neut, Platelet count, =Plt, red blood cell = RBC count, RBC distribution width-variation coefficient = Rdw-cv, RBC distribution width-standard deviation = Rdw-sd, White blood cell count, / μ L = WBC.

Table 2

Comparison of baseline characteristics of participants between study groups.

Investigated trait	Recovered COVID-19 eyes	Healthy eyes	Level statistical significance
age	41.13 \pm 12.6	45.64 \pm 13.7	0.11
Sex (male/ female)	32/19	21/16	0.57
CD ratio	0.19 \pm 0.22	0.24 \pm 0.28	0.41
Spherical equivalent	0.41 \pm 1.5	0.23 \pm 1.3	0.59
Axial length, mm	22.9 \pm 0.7	23.03 \pm 0.6	0.47
Retinal nerve fiber layer thickness (μ m)	115 \pm 16.9	111 \pm 11.8	0.231

cup disk ratio = CD ratio.

Comparison of circumpapillary vessel density (cpVD) and retinal nerve fiber layer (RNFL) thickness value.

and 35 (39.78%) females. The age range was between 9 and 67 years with a mean age of 43.03 years (SD: 13.24). There was no statistically significant difference in age or gender between the recovered COVID-19 patients and the healthy controls. Thirty-two (62.7%) of the recovered COVID-19 patients, and 21 (56.75%) of the healthy participants were male ($p = 0.57$). The time between the initial onset of symptoms and ophthalmologic examination was 63.31 \pm 15.21 (40- 95 days). A complete ophthalmologic examination was performed one month after the patients were discharged with recovery, and Polymerase Chain Reaction (RT-PCR) negativity was confirmed.

The majority of the eyes, 79 (89.77%), had normal vision (VA 20/ 20), and eight eyes (10.22%) had mild visual impairment (VA 20/ 25–20/30) due to uncorrected refractive error or cataracts. The recovered COVID-19 eyes were examined 40–95 days after COVID-19 symptom onset. None of the recovered COVID-19 eyes had related ocular disorders. None of the recovered COVID-19 patients had symptoms or signs of intraocular inflammation, and the examination of the anterior segments and dilated fundus examination were within the normal range.

The structural OCT of the normal and the recovered COVID-19 eyes did not obtained from OCTA, showed clear and organized microvascular networks in the two groups without any blood flow alterations, vessel tortuosity and dropout, vasodilation, vascular remodeling, microaneurysms, looser networks with larger and sparser mesh.

Descriptive measures for peripapillary parameters in both study groups are summarized in Table 3. Patients recovered from COVID-19 had increased peripapillary RNFL (superior, inferior, and temporal quadrants) compared with healthy cases ($P = 0.002$). None of the optic disk vessel density parameters (except the whole image) was statistically significantly between the groups. A good correlation was found between the peripapillary capillary density and peripapillary retinal nerve fiber layer thickness in the recovered COVID-19 patients eyes ($r = 0.45$, $P = 0.001$), and in healthy eyes ($r = 0.4$, $P = 0.03$).

Table 4 shows the comparisons of macular parameters in both study groups. Inner retinal thickness in parafoveal (nasal, inferior), and perfoveal (superior, nasal, inferior) regions were thicker in recovered COVID-19 patients compared to healthy cases, but outer retinal thickness in perfoveal (superior, inferior, temporal) region was thinner in recovered COVID-19 patients compared to healthy subjects. Superficial and deep macular vessel densities except foveal region were statistically higher in recovered COVID-19 patients compared to healthy subjects ($p < 0.001$) after adjustment for age, gender, axial length, and signal strength index.

Figs. 1 and 2, presents the correlation between superficial vessel density (SVD), deep vessel density (DVD), and foveal thickness (inner, outer, and total). SVD, DVD correlated significantly with the foveal thickness (inner, outer, and total) (all $p > 0.05$) in recovered COVID-19 patients, but in healthy eyes, this correlation was between SVD, DVD,

Table 3

Between Recovered COVID-19 patients and healthy eyes. Adjusted p value: Adjusted for age, gender, axial length and signal strength index. . P values <0.05 are shown in bold.

Investigated trait	healthy . A (n = 37)	Recovered COVID-19. B (n = 51)	Recovered COVID-19 ≤ 62 days. C (n = 30)	Recovered COVID-19 >62 days. D (n = 21)	P value A vs B (Adjusted)	P value A VS C (Adjusted)	P value A vs D (Adjusted)
pRNFL Thickness	109± 6.8	115±17.3	114±17.1	116.5 ± 18.3	0.1 (0.002)	0.51 (0.06)	0.15 (0.05)
Superior	128±12.7	138.4 ± 27.4	137.1 ± 23.2	139.6 ± 34.8	0.09 (<0.001)	0.16 (0.04)	0.11 (0.002)
Nasal	100±26.8	108±21.6	103.8 ± 24.6	114.3 ± 15.3	0.17 (0.14)	0.67 (0.45)	0.04 (0.18)
Inferior	136±16.4	144.2 ± 22.5	143±22.02	147.4 ± 24.6	0.12 (<0.001)	0.19 (0.03)	0.06 (0.003)
Temporal	75.6 ± 9.4	75.4 ± 10.9	77.9 ± 9.8	71.6 ± 12.4	0.93 (0.01)	0.37 (0.29)	0.23 (0.01)
Whole image VD	49.67±3.07	49.14±2.7	49.3 ± 2.9	48.3 ± 2.08	0.43 (0.02)	0.45 (0.12)	0.05 (0.11)
Inside disk VD	48.6 ± 7.2	49.36±4.8	49.01±4.9	49.7 ± 5.09	0.6 (0.18)	0.89 (0.25)	0.61 (0.37)
Peripapillary VD	51.5 ± 3.8	51.29±3.4	51.6 ± 3.6	50.1 ± 2.9	0.74 (0.06)	0.86 (0.31)	0.12 (0.12)
Superior VD	51.6 ± 5.8	49.61±5.36	50.1 ± 5.7	48.05±4.4	0.13 (0.05)	0.24 (0.24)	0.1 (0.05)
Nasal VD	51.6 ± 5.9	52.1 ± 5.17	52.5 ± 5.5	51.4 ± 5.04	0.7 (0.31)	0.57 (0.73)	0.87 (0.22)
Inferior VD	53.9 ± 6.7	52.67±4.7	53.6 ± 3.7	50.7 ± 5.8	0.36 (0.07)	0.76 (0.07)	0.17 (0.26)
Temporal VD	50.5 ± 7.03	51.02±5.7	51.07±6.5	50.1 ± 4.2	0.76 (0.37)	0.98 (0.6)	0.61 (0.63)

and inner foveal thickness and total foveal thickness.

5. Discussion

Coronaviruses are known to involve organs and systems other than the respiratory tract, including the digestive system, nervous system, and ocular tissues [12, 13]. Previous reports, suggest ocular infection in the recent SARS-CoV-2 epidemic, and ocular transmission might be a potential route of SARS-CoV-2 infection [14,15]. Despite the fact that several months have gone by since the epidemic, not much has been published with regards to the mechanisms of pathogenicity of SARS-CoV-2, especially with respect to the ocular tissues. In his study we evaluated the ocular findings detected in the recovered COVID-19 patients, using clinical examination, OCT, and OCT angiography imaging, after a mean time of two months, which were compared with normal population.

In this study of 51 patients with confirmed COVID-19 infection, it is noteworthy to say that all 51 patients (100%) had a normal ophthalmology examination and imaging.

None of the recovered COVID –19 patients had ocular or retinal findings. Visual acuity, and pupillary reflexes were normal in all eyes, and we did not detect any symptoms or signs of intraocular inflammation. Our study indicates that patients recovered from COVID-19 have significantly greater superficial and deep macular VD (except foveal region) than healthy subjects, and overall no differences were observed between the shorter and the longer recovery times(Table 3,4).

Previous studies of the state of the retinal vascularisation in patients after COVID-19 are summarized in Table 5. Some researches have reported a reduction in retinal VD, and other vascular parameters of OCTA in adults with SARS-CoV-2 infection [4.5.6.8.9], and one study [7] reported that unaltered macula and perimacular vessel density and perfusion in mild post-COVID-19 patients at 1-month hospital discharge.

These different findings could be attributable to the different periods between acute infection, and ophthalmological examination. In our study, inner macular thickness is higher in eyes with the shorter recovery times, and this study revealed that the frequency of ocular findings might be related to infection time, as the mean time from onset of COVID-19 infection to ophthalmology examination was 63 days (40 to 95 days) in our patients. Among these studies in recovered patients,

the time from onset of infection to ophthalmology examination was not the same, and no longer than one month (between 1 week and one month), which might have led to the higher number of retina findings.

In Zapata report [9], mean days from PCR-confirmed diagnosis to ophthalmological examination time was 72 days in moderate disease, and 70 days in severe disease, which it is almost the same as our study. The discrepancy may be due to the difference in disease severity, differences in the OCT devices, and image processing techniques and analysis. Also, in our study, for evaluated the net retinal effect of COVID-19, we excluded the comorbidity diseases (smoking, diabetes history, or treatment with ACE inhibitors) which affect vascular density, and patients who need ICU care, but in the past study all of the patients included in the study. Importantly, our recovered COVID- 19 subjects are significantly higher than the aforementioned report; besides we have a comparative control healthy populations before the COVID-19 pandemic. In our study, increased of superficial and deep vessels was observed in recovered COVID-19 subjects compared to healthy control, after adjustment for confounders.

In Cennamo, and associates study [10], the median age of patients was older than our study, while advanced age affects the vascular density.

Asikgarip and colleagues [12] recently reported that retinal arteries and veins diameters were significantly increased in COVID-19 patients during the acute phase of the disease compared with healthy controls. vascular enlargement in other organs, such as the pulmonary arteries has been also evidenced[13–14].

Endothelial damage and vessel dilation may be related to the increase in inflammatory cytokines during the infection. An association of inflammatory markers with larger retinal venular diameter, documented in the Beaver Dam Eye Study [15]. It seems, this retinal vascular dilation in COVID-19 patients translates into the presence of a higher retinal VD found by OCTA .

COVID-19 endothelitis can contribute to microcirculatory impairment and clinical sequelae, such as thrombosis and ischemia, cerebrovascular complications in younger patients, myocardial ischemia, and micro-and macrocirculatory thromboembolic complications that can be explained by the endotheliopathy [16–18].

Vascular abnormalities in OCT angiography were rare in COVID –19 participants, which can be an underestimation; whereas vascular

Table 4

Comparison of macular vessel density (VD) and retinal nerve fiber layer (RNFL) thickness values between recovered COVID-19 eyes and healthy eyes.

P value A vs D (Adjusted)	P value A vs C (Adjusted)	P value A vs B (Adjusted)	Recovered COVID-19 >62 days .D	Recovered COVID-19 ≤ 62 days. C	Recovered COVID-19. B	Healthy .A	Investigated trait
Inner macular thickness(μm) (ILM-IPL)							
0.47 (0.67)	0.12 (0.17)	0.47 (0.66)	56.5 ± 7.09	62.8 ± 12.7	60.3 ± 11.01	58.0.2 ± 10.4	Fovea
0.72 (0.09)	0.03 (0.008)	0.23 (0.11)	100.2 ± 7.3	103.9 ± 8.1	101.9 ± 8.2	99.7 ± 8.5	Temporal Parafovea
0.61 (0.18)	0.47 (0.1)	0.81 (0.25)	109.05±9.07	112.5 ± 16.02	111.1 ± 13.4	110±8.5	Superior Parafovea
0.83 (0.09)	0.28 (0.005)	0.73 (0.03)	106.5 ± 9.1	110.3 ± 11.05	108.5 ± 10.34	107±12	Nasal Parafovea
0.66 (0.16)	0.13 (0.006)	0.32 (0.03)	110.1 ± 9.2	113±9.15	111.4 ± 9.1	109±13.9	Inferior Parafovea
0.94 (0.32)	0.73 (0.31)	0.94 (0.59)	86.3 ± 7.6	87.3 ± 8.7	86.8 ± 8.06	86.7 ± 9.3	Temporal Perifovea
0.71 (0.006)	0.52 (<0.001)	0.75 (0.001)	98.1 ± 8.4	100.5 ± 8.7	99.7 ± 8.3	99±9.4	Superior Perifovea
0.92 (0.07)	0.61 (0.002)	0.83 (0.007)	116.2 ± 12.1	117.4 ± 11.1	116.7 ± 11.1	116±12.9	Nasal Perifovea
0.28 (0.03)	0.55 (0.001)	0.33 (0.003)	99.05±10.3	96.9 ± 10.2	97.6 ± 9.95	95.03 ±14.2	Inferior Perifovea
Outer macular thickness (μm) (INL-RPE)							
0.75 (0.41)	0.9 (0.82)	0.87 (0.42)	193.5 ± 12.3	191.7 ± 18.6	191.7 ± 23.1	192.4 ± 15.9	Fovea
0.12 (0.1)	0.89 (0.19)	0.73 (0.07)	216.6 ± 8.9	208.7 ± 36.7	209.8 ± 18.4	211.8 ± 28.8	Temporal Parafovea
0.1 (0.07)	0.07 (0.16)	0.04 (0.06)	221.5 ± 6.5	221.7 ± 14.5	214.3 ± 18.6	221.1 ± 11.9	Superior Parafovea
0.17 (0.19)	0.29 (0.29)	0.19 (0.16)	221.7 ± 9.2	220.1 ± 16.4	215.7 ± 18.5	220.3 ± 13.7	Nasal Parafovea
0.23 (0.26)	0.09 (0.18)	0.08 (0.06)	216.5 ± 7.1	218.2 ± 14.4	211.6 ± 17.5	217.2 ± 11.9	Inferior Parafovea
0.08 (0.01)	0.06 (0.09)	0.04 (0.02)	188±12.5	187.43±12.7	181.5 ± 13.2	187.3 ± 12.2	Temporal Perifovea
0.34 (0.09)	0.25 (0.05)	0.18 (0.03)	189.5 ± 6.3	189.4 ± 8.1	186.1 ± 14.1	189.3 ± 7.3	Superior Perifovea
0.86 (0.7)	0.47 (0.14)	0.66 (0.36)	186.2 ± 13.9	188±13.1	185.8 ± 13.9	187.1 ± 12.9	Nasal Perifovea
0.58 (0.17)	0.17 (0.03)	0.31 (0.017)	178.8 ± 8.006	181.2 ± 10.8	177.44±13.05	180±9.7	Inferior Perifovea
0.08 (0.01)	0.06 (0.09)	0.04 (0.02)	188±12.5	187.43±12.7	181.5 ± 13.2	187.3 ± 12.2	Temporal Perifovea
Total macular thickness (μm)							
0.99 (0.83)	0.52 (0.61)	0.66 (0.57)	250.1 ± 18.4	254.6 ± 28.8	252±24.5	250±27.5	Fovea
0.16 (0.2)	0.61 (0.14)	0.49 (0.08)	316.9 ± 13.2	312.7 ± 38.7	313±30.6	309±22.8	Temporal Parafovea
0.27 (0.2)	0.05 (0.02)	0.07 (0.06)	330.6 ± 14.004	334.3 ± 17.8	332±16.23	332±16.3	Superior Parafovea
0.36 (0.26)	0.15 (0.04)	0.22 (0.12)	328.2 ± 15.8	330.4 ± 18.6	328±17.3	323±24.5	Nasal Parafovea
0.25 (0.19)	0.02 (0.01)	0.057 (0.02)	326.6 ± 14.1	331.2 ± 16.6	328±15.7	320±23.4	Inferior Parafovea
0.19 (0.06)	0.11 (0.04)	0.11 (0.04)	274.3 ± 14.6	274.7 ± 15.3	274±14.6	268±18.1	Temporal Perifovea
0.63 (0.01)	0.26 (0.002)	0.3 (0.007)	287.7 ± 12.9	290.03±14.6	289±13.5	285±19.1	Superior Perifovea
0.86 (0.22)	0.42 (0.03)	0.66 (0.2)	302.5 ± 19.9	305.4 ± 17.4	303±17.8	301±21.4	Nasal Perifovea
0.24 (0.02)	0.12 (0.003)	0.14 (0.005)	277.9 ± 14.9	278.1 ± 12.06	277±12.8	272±18.5	Inferior Perifovea
Superficial vessel density							
0.73 (0.002)	0.21 (<0.001)	0.5 (<0.001)	48.4 ± 4.7	50.21±3.9	49.5 ± 4.2	48.8 ± 4.1	Whole image
0.32 (0.44)	0.07 (0.37)	0.08 (0.67)	21.1 ± 6.3	23.3 ± 10.5	22.5 ± 9.08	19.02±7.7	Fovea
0.86 (<0.001)	0.22 (<0.001)	0.49 (<0.001)	51.6 ± 6.05	53.4 ± 3.7	52.7 ± 4.7	51.9 ± 5.3	Parafovea VD
0.94 (0.002)	0.18 (<0.001)	0.14 (<0.001)	51.7 ± 5.1	53.4 ± 3.4	53.05±4.3	51.4 ± 5.08	Temporal Parafovea VD
0.71 (0.01)	0.7 (0.007)	0.57 (0.002)	52.2 ± 7.04	53.3 ± 4.4	53.1 ± 5.5	52.4 ± 5.3	Superior Parafovea VD
			51.02±6.2	53.08±3.7	52.4 ± 5.02	51.2 ± 5.4	

(continued on next page)

Table 4 (continued)

P value A vs D (Adjusted)	P value A vs C (Adjusted)	P value A vs B (Adjusted)	Recovered COVID-19 >62 days .D	Recovered COVID-19 ≤ 62 days. C	Recovered COVID-19. B	Healthy .A	Investigated trait
0.76 (0.001)	0.22 (0.002)	0.28 (<0.001)					Nasal Parafovea VD
0.93 (0.005)	0.51 (0.001)	0.41 (0.002)	51.6 ± 7.2	52.6 ± 4.1	52.5 ± 5.4	51.4 ± 6.1	Inferior Parafovea VD
0.75 (0.003)	0.3 (<0.001)	0.58 (<0.001)	49.006±4.7	50.6 ± 4.02	50±4.3	49.4 ± 4.5	Perifovea
0.82 (0.01)	0.94 (0.006)	0.34 (0.003)	46.6 ± 5.4	47.06±3.6	47.3 ± 4.9	46.2 ± 4.2	Temporal Perifovea VD
0.27 (0.003)	0.7 (<0.001)	0.72 (<0.001)	48.1 ± 5.2	50.1 ± 3.5	49.7 ± 4.4	49.3 ± 4.5	Superior Perifovea VD
0.44 (0.008)	0.56 (0.02)	0.42 (0.008)	52.2 ± 4.3	53.7 ± 3.7	53.5 ± 4.1	52.7 ± 3.5	Nasal Perifovea VD
0.89 (0.05)	0.33 (0.02)	0.08 (0.002)	48.9 ± 4.5	49.8 ± 3.5	49.8 ± 4.3	48.1 ± 3.8	Inferior Perifovea VD
Deep vessel density							
0.39 (<0.001)	0.69 (<0.001)	0.47 (<0.001)	51.6 ± 6.9	50.4 ± 5.3	50.9 ± 5.8	49.8 ± 7.2	whole image VD
0.95 (0.37)	0.14 (0.52)	0.28 (0.94)	38.5 ± 6.2	41.2 ± 6.9	40.2 ± 6.6	38.4 ± 7.9	Fovea VD
0.46 (<0.001)	0.64 (<0.001)	0.46 (<0.001)	55.9 ± 4.7	55.2 ± 4.8	55.4 ± 4.7	54.4 ± 7.3	Parafovea VD
0.8 (<0.001)	0.95 (<0.001)	0.87 (<0.001)	56.7 ± 4.6	56.4 ± 4.3	56.5 ± 4.3	56.3 ± 6.2	Temporal Parafovea VD
0.2 (<0.001)	0.83 (<0.001)	0.42 (<0.001)	56.8 ± 4.4	54.6 ± 5.39	55.4 ± 5.08	54.3 ± 7.2	Superior Parafovea VD
0.49 (<0.001)	0.6 (<0.001)	0.46 (<0.001)	57.2 ± 4.3	56.8 ± 4.8	56.9 ± 4.5	56±6.2	Nasal Parafovea VD
0.42 (<0.001)	0.96 (<0.001)	0.7 (<0.001)	54.9 ± 5.8	53.05±6.1	53.7 ± 5.9	53.1 ± 8.2	Inferior Parafovea VD
0.25 (<0.001)	0.59 (<0.001)	0.33 (<0.001)	53.4 ± 7.1	51.8 ± 6.3	52.4 ± 6.6	50.8 ± 7.8	Perifovea
0.43 (<0.001)	0.88 (<0.001)	0.61 (<0.001)	55.6 ± 5.1	54.4 ± 5.5	54.8 ± 5.3	54.1 ± 6.6	Temporal Parafovea VD
0.42 (<0.001)	0.76 (<0.001)	0.53 (<0.001)	52.01±7.6	50.6 ± 6.9	51.1 ± 7.07	50.08±7.9	Superior Parafovea VD
0.36 (<0.001)	0.86 (<0.001)	0.57 (<0.001)	52.4 ± 8.8	50.5 ± 7.4	51.2 ± 7.8	50.1 ± 7.5	Nasal Parafovea VD
0.12 (<0.001)	0.59 (<0.001)	0.25 (<0.001)	54.3 ± 7.5	51.5 ± 7.07	52.5 ± 7.2	50.5 ± 7.7	Inferior Parafovea VD
0.45 (0.92)	0.21 (0.54)	0.15 (0.71)	0.277±0.6	0.24±0.1	0.25±0.08	0.37±0.53	FAZ area
0.23 (0.61)	0.4 (0.52)	0.96 (0.76)	2.09±0.31	1.87±.41	1.9 ± 0.38	1.9 ± 0.39	Perim
0.02 (0.1)	0.15 (0.39)	0.06 (0.27)	1.11±0.09	1.08±0.03	1.09±0.06	1.07±0.02	Ai
0.7 (0.001)	0.43 (<0.001)	0.76 (<0.001)	53.37±6.57	55.21±4.604	54.5 ± 5.4	54.1 ± 6.03	FD
0.15 (0.35)	0.01 (0.1)	0.09 (0.13)	2.03±.48	1.9 ± 0.58	2.01±0.46	2.1 ± 0.1	CCF area
0.67 (0.86)	0.83 (0.33)	0.8 (0.18)	98.8 ± 9.4	100.3 ± 10.2	99.88±9.9	99.7 ± 9.7	GCL

Adjusted p value: Adjusted for age, gender, axial length and signal strength index.

Foveal avascular zone=FAZ, FAZ perimeter (PERIM), choriocapillary flow area (CCF), acircularity index (AI), foveal density (FD) . . P values <0.05 are shown in bold.

variations can be detected, using fluorescein angiography that allows for a dynamic assessment of the retinal and choroidal vasculature.

In our study, of FAZ metrics, only foveal vessel density (FD) showed significant differences between the two groups (greater in the recovered COVID-19 group)($p < 0.001$). In COVID-19 adults, Turker and colleagues [4] found that the FAZ area was greater in the COVID group than in the control group, but this did not reach statistical significance. Contrary to this study, the FAZ area was lower in recovered COVID-19 patients than healthy cases, but this difference was not statistically significant.

The present study found a significant difference in the average and sectoral peripapillary RNFL between the two groups. In addition, retinal thickness was evaluated, and recovered COVID-19 patients had higher inner retinal thickness (perifovea and parafovea), and lower outer retinal thickness (perifovea) compared to healthy cases.

Oren et al. [19] also demonstrated alterations in the retinal thickness, including a significantly higher central macular thickness, thinner ganglion cell layer, and inner nuclear layer in patients recovered from

COVID-19.

In contrary to this study, peripapillary RNFL thickness after adjustment for confounding factors was higher in recovered COVID-19 patients compared to healthy eyes. A possible explanation for their contradictory results might be that these investigations did not excluded any systemic illnesses, including diabetic mellitus or medications that might affect the retina, and these studies did not present the SSI adjusted comparison. Recent reports have shown a reduction in vessel density in older age and lower scan quality, and this must be addressed in the analysis [20–23].

Barbara Burgos-Blasco et al. [24] reported an increase of peripapillary rNFL thickness (global and sectoral) in recovered children COVID-19 patients.

The retina is an extension of the brain and retinal anatomy, function, response to injury, and immune responses similarly to those in the brain and spinal cord. A retinal ganglion cell (RGC) is a type of neuron located in the ganglion cell layer of the retina and in the thalamic region form

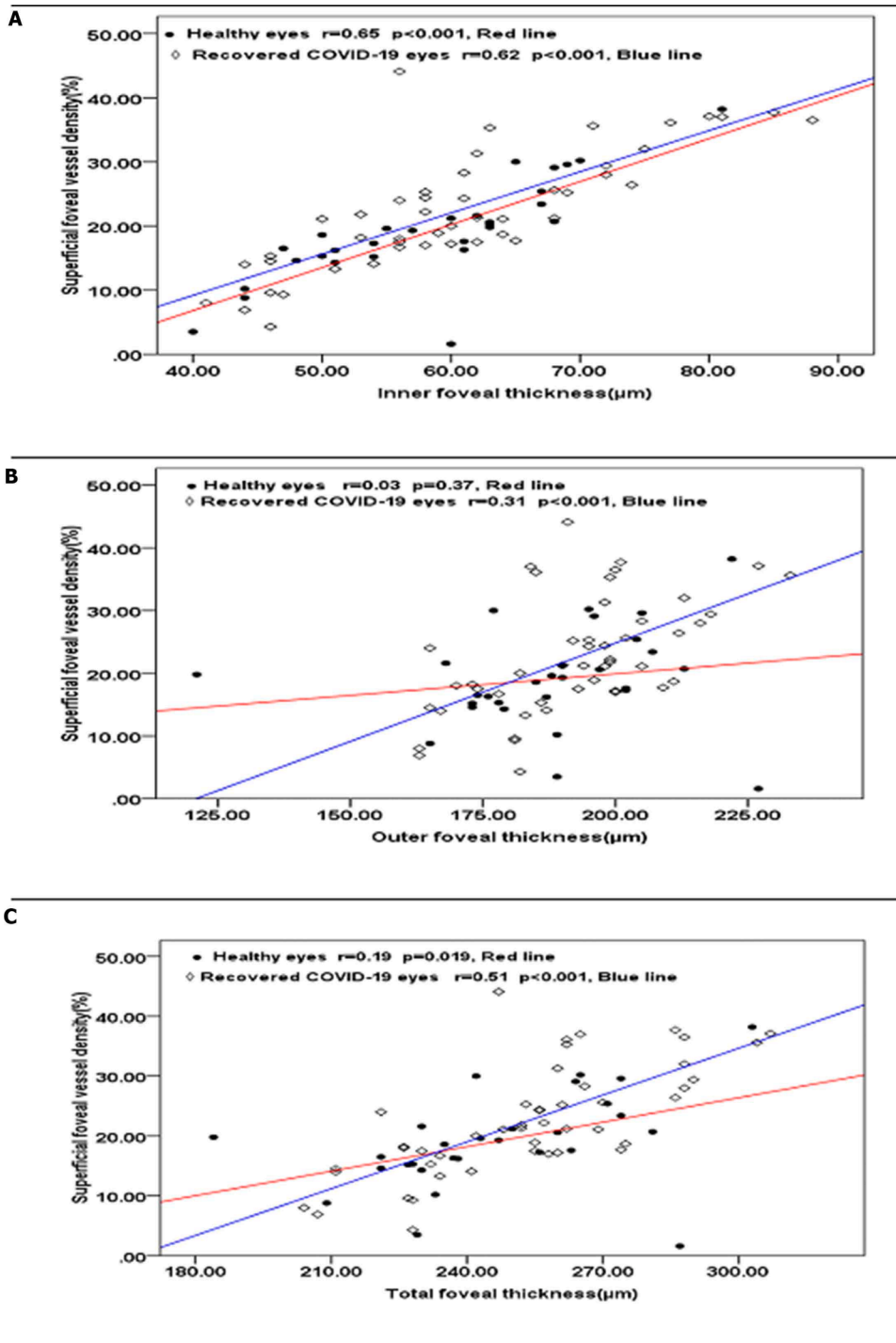


Fig. 1. Correlation of vessel density (VD) of the superficial capillary plexus (SCP) with inner, outer and total foveal thickness in recovered COVID-19 eyes and healthy normal eyes (Pearson correlation). The overall VD correlated positively with foveal thickness in both the recovered COVID-19 eyes and normal eyes. A significant correlation was found between the VD and inner, outer, and total foveal thickness in recovered COVID-19 eyes. In healthy normal eyes, a significant correlation was found between the VD and inner, and total foveal thickness.

direct synaptic connections with the CNS [25].

Ganglion cell and plexiform layer might be associated with central nervous system manifestations that were previously described in animal studies and COVID-19 neurological findings [26–27].

The macula has the highest density of (retinal ganglion cells) RGCs, which exist in the inner retinal layer, and gets its oxygen supply from superficial retinal capillary plexuses [28–29]. The retinal thickness and vessel density in the foveal region is higher in recovered COVID-19 patients versus the healthy subject, but it was not statistically significant.

Increased peripapillary and macular vessel density, was reported in recovered children 4- 8 weeks after COVID-19 infection [30]. The

methodology of this study was similar to our study, and used healthy historical control and not including severe and critical patients.

We think that all the vasculature in the body might be changed during/after Covid-19 infection, i.e., not just the eye vasculature but other vasculature as well. Several studies have highlighted the presence of a substantial vascular component in the pathophysiology of the disease [31–34]. Presumably heavy Covid-19 infection causes a lack of oxygen in the body, possibly releasing hypoxia-inducible factor 1 (HIF-1) alpha, and hence Vascular Endothelial Growth Factor A (VEGFA).

To the best of our knowledge, this is the first study to assess the ocular findings of COVID-19 patients without comorbidities after recovery to 3 months in West Asian Patients. It is worth noting that our

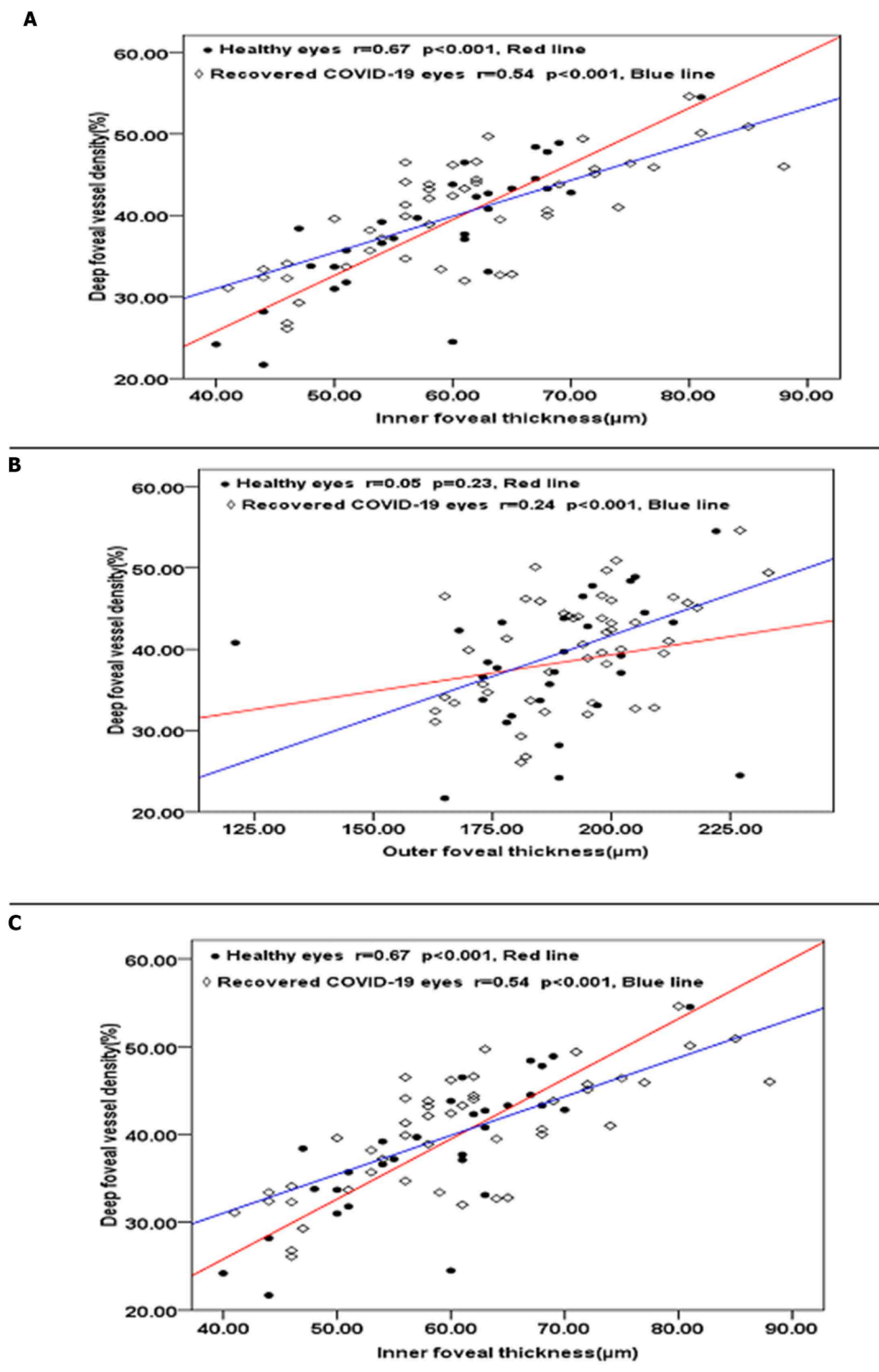


Fig. 2. Correlation of vessel density (VD) of the deep capillary plexus (DCP) with inner, outer and total foveal thickness in recovered COVID-19 eyes and healthy normal eyes (Pearson correlation). The overall VD correlated positively with foveal thickness in both the recovered COVID-19 eyes and normal eyes. A significant correlation was found between the VD and inner, outer, and total foveal thickness in recovered COVID-19 eyes. In healthy normal eyes, a significant correlation was found between the VD and inner, and total foveal thickness.

groups were matched in terms of age and gender, and historical control participants examination and imaging were performed before the COVID-19 outbreak.

The latest version of built-in software was used in this study, which automatically provides VD at various retinal layers, and removes large vessels from peripapillary images. Also, our regional analysis coverage of the involved area is higher, using a large scan size (whole6 × 6mm²scanning field). We adjusted SSI value and other covariates, which yielded the finding that VDs were increased in recovered COVID-19

patients.

This study has several limitations, and the main one is the small number of recovered COVID-19 patients, which none of them needed intensive care, as well as the limited follow-up time. Further studies with a larger sample size are required to reassess our findings. Another limitation is that all of the patients were of Iranian origin, which cannot reflect upon the entire population of recovered COVID-19 patients. In addition, some patients may have received medical intervention once they were suspected of having or confirmed to have an infection, which

Table 5
Previous studies of retinal finding in recovered COVID-19 patients using OCT angiography.

study	patients	Disease severity	Study time	OCT angiography machine	results
Turker et al. ⁴	54 eyes of 27 patients 54 healthy eyes (volunteers for routine ophthalmologic examination)	All patients were hospitalized	within 1 week of discharge after complete recovery as indicated with conversion to PCR-negative status	AngioVue Imaging System versio 2017.1 (Optovue, Inc, Fremont, Calif).	Reduced vessel density of the retinal capillary plexus was detected in COVID-19 patients who may be at risk for retinal vascular complications.
Abrishami et al. ⁵	31 recovered COVID-19 patients 23 healthy normal controls (2019 as part of a prior study to build a local OCTA normative database)	Mild to moderate 29% hospitalized No intubation	at least 2 weeks after recovery from systemic COVID-	AngioVue (RTVue XR Avanti, Optovue, Fremont, Calif; Software Version 2018.0.0.14)	Patients recovered from COVID-19 displayed alterations in the retinal microvasculature, including a significantly lower VD in the SCP and DCP. Patients with coronavirus infection may be at risk of retinal vascular complications
González-Zamora et al. ⁶	50 eyes (25 patients and 25 controls)	Hospitalized patients	14 days after hospital discharge	(DRI OCT Triton SS-OCT Angio, Topcon Medical Systems, Inc. Oakland, NJ, USA)	COVID-19 patients presented significantly thinner ganglion cell layer (GCL) ($p = 0.003$) and thicker retinal nerve fiber layer (RNFL) compared to controls ($p = 0.048$), In both SCP and DCP, COVID-19 patients presented lower VD in the foveal region ($p < 0.001$) and a greater FAZ area than controls ($p = 0.007$).
Savastano et al. ⁷	70 post-COVID-19 patients 22 healthy control subjects.	hospitalized patients	1-month hospital discharge and	OCT and OCTA analysis (Zeiss Cirrus 5000-HD-OCT Angioplex, sw version 10.0, Carl Zeiss, Meditec, Inc., Dublin, USA).	Macula and perimacular vessel density and perfusion resulted unaltered in mild post-COVID-19 patients at 1-month hospital discharge, suggesting no or minimal retinal vascular involvement by SARS-CoV-2.
Hazar L ⁸	50 patients with SARS CoV2 pneumonia 55 healthy age- and gender-matched controls were compared using OCTA.	mild to moderate pneumonia	one month after the patients were discharged with recovery, and PCR negativity was confirmed	AngioVue OCTA device (Optovue, Fremont, CA; software version 2016.2.0.35)	In COVID-19 disease, VD is low in some sectors in both SF and deep layers, but no change in FAZ.
Zapata ⁹	Results Control group included 27 subjects: group 1 included 24 patients, group 2 consisted of 24 patients and 21 participants were recruited for group 3	Mild Moderate Severe	Mean days from PCR-confirmed diagnosis to ophthalmological examination time were 72 and 70 days (group 2 and group 3, respectively).	DRI OCT Triton Swept Source (Topcon Corporation, Tokyo, Japan)	Patients with moderate and severe SARS-CoV-2 pneumonia had decreased central retinal VD as compared with that of asymptomatic/ paucisymptomatic cases or control subjects.
Cennamo G ¹⁰	40 patients post-SARS-CoV-2 infection 40 healthy subjects	moderate illness	6 months from discharge	OCTA scanning. (Optovue Angiovue System, software ReVue XR version 2017.1.0.151, Optovue Inc., Fremont, California, USA)	OCTA showed retinal vascular changes in subjects fully recovered from COVID-19 pneumonia. These findings could be a consequence of a thrombotic microangiopathy that affected retinal structures as well as other systemic organs. OCTA could represent a valid, noninvasive biomarker of early vascular dysfunction after SARS-CoV-2 infection.

could have affected the ocular findings, but this was not accounted for in this study. Since BCVA of 20/40 or better were used, this might have skewed the outcomes, and would potentially introduce bias, and select for patients with less disease. Finally, OCT-A is a relatively new technique, and its limitations must be considered. Apart from the artifacts, the obtained images and data analyzing techniques, might in fact lead to different results, and must be taken into account when comparing the results of different studies.

In conclusion, the recovered COVID19 patients without comorbidity had higher superficial and deep macular VDs in comparison with the healthy eyes matched for age and gender, two to three months after infection. The results suggest that the pathogenic mechanisms affecting vascular damage may be involved in the eyes' tissue. Finally, the theory that vascular changes in COVID -19 are significant should be further investigated in larger prospective studies.

Ethics approval and consent to participate

The Isfahan university of medical sciences approved this study .This

study followed the tenets of the Declaration of Helsinki.

Consent for publication

This manuscript does not contain any individual patient data

Availability of data and materials

Not applicable.

Funding

The author declares that no funding or research Grant was obtained for this manuscript.

Declaration of Competing Interest

The author declares that he has no competing interest

Acknowledgement

Very special thanks to Mr. Hassan Hoseinifard, Ms. Nayyer Danesh, Ms. Mahin Mohammadi, Ms. Pegah Noorshargh, Ms Fariba Naderi Beni and Ms Safoura Hoseinzadeh for all your help and support.

References

- [1] P. Wu, F. Duan, C. Luo, Q. Liu, X. Qu, L. Liang, et al., Characteristics of ocular findings of patients with coronavirus disease 2019 (COVID-19) in Hubei Province, China, *JAMA Ophthalmol.* 138 (5) (2020 May) 575–578, <https://doi.org/10.1001/jamaophthalmol.2020.1291>. PMID: 32232433; PMCID: PMC7110919.
- [2] P.M. Mariño, A.A.A. Marcos, A.C. Romano, H. Nascimento, R. Belfort Jr., Retinal findings in patients with COVID-19, *Lancet* 395 (10237) (2020 May) 1610, [https://doi.org/10.1016/S0140-6736\(20\)31014-X](https://doi.org/10.1016/S0140-6736(20)31014-X). Epub 2020 May 12. PMID: 32405105; PMCID: PMC7217650.
- [3] M.F. Landecho, J.R. Yuste, E. Gándara, COVID-19 retinal microangiopathy as an in vivo biomarker of systemic vascular disease? *J. Intern. Med.* (2020). -07-30.
- [4] I.C. Turker, C.U. Dogan, D. Guven, O.K. Kutucu, C. Gul, Optical coherence tomography angiography findings in patients with COVID-19, *Can. J. Ophthalmol.* 56 (2) (2021 Apr) 83–87, <https://doi.org/10.1016/j.cjco.2020.12.021>. Epub 2021 Jan 9. PMID: 33497612; PMCID: PMC7833266.
- [5] M. Abrishami, Z. Emamveridian, N. Shoebi, A. Omidtabrizi, R. Daneshvar, T. Saedi Rezvani, et al., Optical coherence tomography angiography analysis of the retina in patients recovered from COVID-19: a case-control study, *Can. J. Ophthalmol.* 56 (1) (2021 Feb) 24–30, <https://doi.org/10.1016/j.cjco.2020.11.006>. Epub 2020 Nov 14. PMID: 33249111; PMCID: PMC7666612.
- [6] J. González-Zamora, V. Bilbao-Malavé, E. Gándara, A. Casablanca-Piñera, C. Boquera-Ventosa, M.F. Landecho, et al., Retinal microvascular impairment in COVID-19 bilateral pneumonia assessed by optical coherence tomography angiography, *Biomedicine* 9 (3) (2021 Mar) 247, <https://doi.org/10.3390/biomedicine9030247>. PMID: 33801324; PMCID: PMC7999142.
- [7] M.C. Savastano, G. Gambini, G.M. Cozzupoli, E. Crincoli, A. Savastano, U. De Vico, Against COVID-19 post-acute care study group. Retinal capillary involvement in early post-COVID-19 patients: a healthy controlled study, *Graefes Arch. Clin. Exp. Ophthalmol.* 259 (8) (2021 Aug) 2157–2165, <https://doi.org/10.1007/s00417-020-05070-3>. Epub 2021 Feb 1. PMID: 33523252; PMCID: PMC7848665.
- [8] L. Hazar, M. Karahan, E. Vural, S. Ava, S. Erdem, M.E. Dursun, et al., Macular vessel density in patients recovered from COVID 19, *Photodiagnosis Photodyn. Ther.* 34 (2021 Jun), 102267, <https://doi.org/10.1016/j.pdpdt.2021.102267>. Epub 2021 Mar 27. PMID: 33785439; PMCID: PMC7999941.
- [9] M.Á. Zapata, S. Banderas García, A. Sánchez-Moltalvá, A. Falcó, S. Otero-Romero, G. Arcos, et al., Retinal microvascular abnormalities in patients after COVID-19 depending on disease severity, *Br. J. Ophthalmol.* (2020 Dec), <https://doi.org/10.1136/bjophthalmol-2020-317953> *bjophthalmol-2020-317953*Epub ahead of print; PMID: 33328184; PMCID: PMC7745458.
- [10] G. Cennamo, M. Reibaldi, D. Montorio, L. D'Andrea, M. Fallico, M. Triassi, Optical coherence tomography angiography features in post-COVID-19 pneumonia patients: a pilot study, *Am. J. Ophthalmol.* 227 (2021 Jul) 182–190, <https://doi.org/10.1016/j.ajo.2021.03.015>. Epub 2021 Mar 27. PMID: 33781767; PMCID: PMC7997850.
- [11] A. Naderi Beni, Z. Imani, H. Ghanbari, Comparison of peripapillary and macular vascular density in primary open-angle glaucoma, pseudoexfoliation glaucoma, and normal control eyes, *Photodiagnosis Photodyn. Ther.* 37 (2021 Nov), 102611, <https://doi.org/10.1016/j.pdpdt.2021.102611>. Epub ahead of print; PMID: 34737059.
- [12] N. Aşıkgarip, E. Temel, L. Hızmalı, K. Örnek, F.M. Sezgin, Retinal vessel diameter changes in COVID-19 infected patients, *Ocul. Immunol. Inflamm.* 29 (4) (2021 May) 645–651, <https://doi.org/10.1080/09273948.2020.1853783>. Epub 2021 Jan 26. PMID: 33497297.
- [13] Y. Li, L. Xia, Coronavirus disease 2019 (COVID-19): role of chest CT in diagnosis and management, *AJR Am. J. Roentgenol.* 214 (6) (2020 Jun) 1280–1286, <https://doi.org/10.2214/AJR.20.22954>. Epub 2020 Mar 4. PMID: 32130038.
- [14] P. Spagnolo, A. Cozzi, R.A. Foà, A. Spinazzola, L. Nonfardini, C. Bnà, CT-derived pulmonary vascular metrics and clinical outcome in COVID-19 patients, *Quant. Imaging Med. Surg.* 10 (6) (2020 Jun) 1325–1333, [10.21037/qims-20-546](https://doi.org/10.21037/qims-20-546). PMID: 32550141; PMCID: PMC7276354.
- [15] R. Klein, B.E. Klein, M.D. Knudtson, T.Y. Wong, M.Y. Tsai, Are inflammatory factors related to retinal vessel caliber? The Beaver Dam Eye Study, *Arch. Ophthalmol.* 124 (1) (2006 Jan) 87–94, <https://doi.org/10.1001/archophth.124.1.87>. PMID: 16401789.
- [16] Z. Varga, A.J. Flammer, P. Steiger, M. Haberecker, R. Andermatt, A.S. Zinkernagel, Endothelial cell infection and endotheliitis in COVID-19, *Lancet* 395 (10234) (2020 May) 1417–1418, [https://doi.org/10.1016/S0140-6736\(20\)30937-5](https://doi.org/10.1016/S0140-6736(20)30937-5). Epub 2020 Apr 21. PMID: 32325026; PMCID: PMC7172722.
- [17] T. Iba, J.H. Levy, J. Thachil, H. Wada, M. Levi, Scientific and standardization committee on DIC of the international society on thrombosis and haemostasis. The progression from coagulopathy to disseminated intravascular coagulation in representative underlying diseases, *Thromb. Res.* 179 (2019 Jul) 11–14, <https://doi.org/10.1016/j.thromres.2019.04.030>. Epub 2019 Apr 29. PMID: 31059996.
- [18] T. Iba, J.H. Levy, H. Wada, J. Thachil, T.E. Warkentin, M. Levi, Subcommittee on disseminated intravascular coagulation. Differential diagnoses for sepsis-induced disseminated intravascular coagulation: communication from the SSC of the ISTH, *J. Thromb. Haemost.* 17 (2) (2019 Feb) 415–419, <https://doi.org/10.1111/jth.14354>. Epub 2019 Jan 7. PMID: 30618150.
- [19] B. Oren, Aksoy Aydemir G, E. Aydemir, H.I. Atesoglu, Y.S. Goker, H. Kızıltoprak, et al., Quantitative assessment of retinal changes in COVID-19 patients, *Clin. Exp. Optom.* 104 (6) (2021 Aug) 717–722, <https://doi.org/10.1080/08164622.2021.1916389>. Epub 2021 May 20. PMID: 34016010.
- [20] T. Shoji, L.M. Zangwill, T. Akagi, L.J. Saunders, A. Yarmohammadi, P.I. C. Manalastas, et al., Progressive macula vessel density loss in primary open-angle glaucoma: a longitudinal study, *Am. J. Ophthalmol.* 182 (2017 Oct) 107–117, <https://doi.org/10.1016/j.ajo.2017.07.011>. Epub 2017 Jul 20. PMID: 28734815; PMCID: PMC5610624.
- [21] A. Shahlaee, W.A. Samara, J. Hsu, E.A. Say, M.A. Khan, J. Sridhar, In vivo assessment of macular vascular density in healthy human eyes using optical coherence tomography angiography, *Am. J. Ophthalmol.* 165 (2016 May) 39–46, <https://doi.org/10.1016/j.ajo.2016.02.018>. Epub 2016 Feb 24. PMID: 26921803.
- [22] S. Moghimi, L.M. Zangwill, R.C. Pentead, K. Hasenstab, E. Ghahari, H. Hou, Macular and optic nerve head vessel density and progressive retinal nerve fiber layer loss in glaucoma, *Ophthalmology* 125 (11) (2018 Nov) 1720–1728, <https://doi.org/10.1016/j.optha.2018.05.006>. Epub 2018 Jun 12. PMID: 29907322.
- [23] H. Hou, S. Moghimi, L.M. Zangwill, T. Shoji, E. Ghahari, R.C. Pentead, et al., Macula vessel density and thickness in early primary open-angle glaucoma, *Am. J. Ophthalmol.* 199 (2019 Mar) 120–132, <https://doi.org/10.1016/j.ajo.2018.11.012>. Epub 2018 Nov 26. PMID: 30496723; PMCID: PMC6382614.
- [24] B. Burgos-Blasco, N. Güemes-Villaloz, L. Morales-Fernandez, I. Callejas-Caballero, P. Perez-Garcia, J. Donate-Lopez, et al., Retinal nerve fibre layer and ganglion cell layer changes in children who recovered from COVID-19: a cohort study, *Arch. Dis. Child.* (2021 Aug), <https://doi.org/10.1136/archdischild-2021-321803> *archdischild-2021-321803*Epub ahead of print. PMID: 34340983; PMCID: PMC8331319.
- [25] Y. Wang, B. Detrick, Z.X. Yu, J. Zhang, L. Chesky, J.J. Hooks, The role of apoptosis within the retina of coronavirus-infected mice, *Invest. Ophthalmol. Vis. Sci.* 41 (10) (2000 Sep) 3011–3018. PMID: 10967058.
- [26] A. London, I. Benhar, M. Schwartz, The retina as a window to the brain—from eye research to CNS disorders, *Nat. Rev. Neurol.* 9 (1) (2013 Jan) 44–53, <https://doi.org/10.1038/nrneuro.2012.227>. Epub 2012 Nov 20. PMID: 23165340.
- [27] T. Moriguchi, N. Harii, J. Goto, D. Harada, H. Sugawara, J. Takamino, et al., A first case of meningitis/encephalitis associated with SARS-Coronavirus-2, *Int. J. Infect. Dis.* 94 (2020 May) 55–58, <https://doi.org/10.1016/j.ijid.2020.03.062>. Epub 2020 Apr 3. PMID: 32251791; PMCID: PMC7195378.
- [28] J.M. Provis, Development of the primate retinal vasculature, *Prog. Retin. Eye Res.* 20 (2001) 799–821.
- [29] J.P. Campbell, M. Zhang, T.S. Hwang, S.T. Bailey, D.J. Wilson, Y. Jia, Detailed vascular anatomy of the human retina by projection-resolved optical coherence tomography angiography, *Sci. Rep.* 7 (2017 Feb) 42201, <https://doi.org/10.1038/srep42201>. PMID: 28186181; PMCID: PMC5301488.
- [30] N. Güemes-Villaloz, B. Burgos-Blasco, P. Perez-Garcia, J.I. Fernández-Vigo, L. Morales-Fernandez, J. Donate-Lopez, Retinal and peripapillary vessel density increase in recovered COVID-19 children by optical coherence tomography angiography, *J. AAPOS* (2021), <https://doi.org/10.1016/j.jaapos.2021.06.004>. Oct 20: S1091-8531(21)00552-8Epub ahead of print. PMID: 34687877; PMCID: PMC8527103.
- [31] M. Ackermann, S.E. Verleden, M. Kuehnel, A. Haverich, T. Welte, F. Laenger, et al., Pulmonary vascular endothelialitis, thrombosis, and angiogenesis in Covid-19, *N. Engl. J. Med.* 383 (2) (2020 Jul) 120–128, <https://doi.org/10.1056/NEJMoa2015432>. Epub 2020 May 21. PMID: 32437596; PMCID: PMC7412750.
- [32] T. Iba, J.M. Connors, J.H. Levy, The coagulopathy, endotheliopathy, and vasculitis of COVID-19, *Inflamm. Res.* 69 (12) (2020 Dec) 1181–1189, <https://doi.org/10.1007/s00011-020-01401-6>. Epub 2020 Sep 12. PMID: 32918567; PMCID: PMC7486586.
- [33] C. Vacchi, M. Meschiari, J. Milic, M. Marietta, R. Tonelli, G. Alfano, et al., COVID-19-associated vasculitis and thrombotic complications: from pathological findings to multidisciplinary discussion, *Rheumatology (Oxford)* 59 (12) (2020 Dec) e147–e150, <https://doi.org/10.1093/rheumatology/keaa581>. PMID: 32968761; PMCID: PMC7543638.
- [34] L. Verdoni, A. Mazza, A. Gervasoni, L. Martelli, M. Ruggeri, M. Ciuffreda, et al., An outbreak of severe Kawasaki-like disease at the Italian epicentre of the SARS-CoV-2 epidemic: an observational cohort study, *Lancet* 395 (10239) (2020 Jun) 1771–1778, [https://doi.org/10.1016/S0140-6736\(20\)31103-X](https://doi.org/10.1016/S0140-6736(20)31103-X). Epub 2020 May 13. PMID: 32410760; PMCID: PMC7220177.